Pattern Recognition Letters 33 (2012) 1411–1421

Contents lists available at SciVerse ScienceDirect

Pattern Recognition Letters

journal homepage: www.elsevier.com/locate/patrec

Minutia handedness: A novel global feature for minutiae-based fingerprint matching

Kai Cao [a,1], Xin Yang [b,1], Xinjian Chen [c,1], Xunqiang Tao [b], Yali Zang [b], Jimin Liang [a], Jie Tian [a,b,*]

[a] Life Sciences Research Center, School of Life Sciences and Technology, Xidian University, Xi'an 710071, China
[b] Institute of Automation, Chinese Academy of Sciences, Beijing 100190, China
[c] Radiology and Imaging Sciences Department, Clinical Center, National Institute of Health, MD 20892, USA

ARTICLE INFO

Article history:
Received 24 December 2010
Available online 28 March 2012

Communicated by K.A. Toh

Keywords:
Fingerprint matching
Minutia
Minutia handedness
Reference point
Global feature

ABSTRACT

Traditional minutiae-based matching algorithms are challenged by the probability that minutiae from different regions of different fingers may not be well matched, and hence lead to erroneous matching results. In this paper we introduce a novel feature called minutia handedness to deal with this problem. First, reference points are detected and additional checking conditions are added to ensure that genuine and accurate reference points can be found. Second, minutia handedness is defined for each minutia according to the bending degree of its associated ridges or the position of the reference points. There are three types of minutiae handedness: right-handed, left-handed and non-handed. Finally, the matching rules between different types of minutiae handedness are set up. The proposed method is tested on eight data sets of FVC2002 (2002) and FVC2004 (2004). The experimental results indicate that the performance of a convectional fingerprint recognition algorithm can be improved by incorporating minutia handedness with a small increment of template size.

1. Introduction

Fingerprint is much more reliable than most other biometrics such as signature, face and speech (Jain et al., 1997b), and has been widely used in many important applications such as electronic personal identification cards, and e-commerce. However, fingerprint recognition is still a challenging task. The performance of even a state-of-the-art matching algorithm is still much lower than most people's expectations and theory estimation (Pankanti et al., 2002). Therefore, much effort is still needed to improve the performance of the fingerprint recognition system.

Based on the features used in fingerprint matching, most existing algorithms can be classified into two categories: minutiae-based approaches and global feature-based approaches. It is widely believed that minutiae are the most discriminating and reliable features in fingerprints. Many matching methods based on minutiae have been proposed (Maltoni et al., 2009; Jain et al., 1997a). Since the relative transformation between two fingerprints is unknown in advance, the correspondence between minutiae is very ambiguous. Many researchers have tried to attach local features to minutiae to reduce ambiguity. These local features include ridge information (Jain et al., 1997a; He et al., 2003), local orientation features sampled around the minutiae (Tico and Kuosmanen, 2003) and local minutiae structure features (Chen et al., 2006; Ratha et al., 2000). Recently, He et al. (2006) proposed a global comprehensive similarity-based fingerprint matching algorithm, in which a minutiae-simplex, including a pair of minutiae as well as their associated textures, were employed to achieve fingerprint matching. He et al. (2007) extended this approach by representing a fingerprint as a graph, in which the comprehensive minutiae acted as the vertex set and the local binary minutiae relations were used to provide the edge set. Some researchers combined other local features to increase the discriminative ability between minutiae. Feng (2008) combined a texture descriptor and a minutiae descriptor to measure the similarity between minutiae. Wang et al. (2007a) defined two rotation and translation invariant features (OrientationCode and PolyLine) and fused them to calculate the similarity between corresponding minutiae. Local information can even be employed to generate an alignment-free cancelable template (Lee et al., 2007). Although incorporating more discriminative information into minutiae can reinforce the individuality of fingerprints and improve the system performance, two fingerprints from different fingers may contain similar minutiae, orientation and ridge features in a partial region. Fig. 1 shows an example of a pair of fingerprints from FVC2002 DB1. To intuitively solve this problem is to reject the input fingerprint with small overlapping region. However, this approach will result in a large false rejection rate because there may also be a small overlapping region for a genuine match as shown in Fig. 2.

Global features are widely used in identification, indexing (Chang and Fan, 2002) and classification (Shah and Sastry, 2004). Jain et al. (2000) proposed a fingerprint representation called the

* Corresponding author at: Life Sciences Research Center, School of Life Sciences and Technology, Xidian University, Xi'an 710071, China.
E-mail address: tian@ieee.org (J. Tian).
[1] These authors contributed equally to this work.

0167-8655/$ - see front matter © 2012 Elsevier B.V. All rights reserved.
http://dx.doi.org/10.1016/j.patrec.2012.03.007

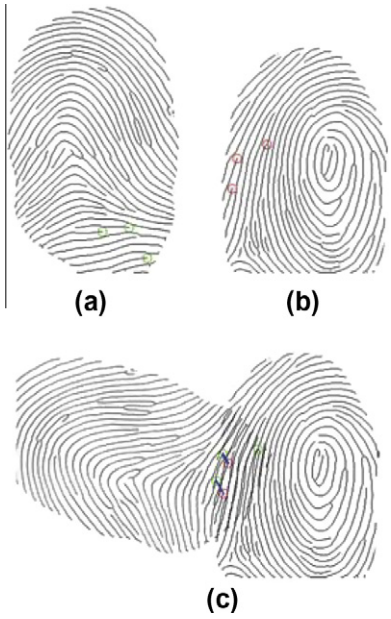

Fig. 1. An example of two fingerprints from FVC2002 DB1. Minutiae from different regions of different fingers are matched very well. The circles denote the matched minutiae: (a) thinned image of 56_1.tif; (b) thinned image of 98_1.tif; (c) registration of (a) and (b).

FingerCode. In this method, a reference point was first detected and a fixed-length feature vector was extracted by using Gabor filters in the region surrounding the reference point to represent the fingerprint. Lee and Wang (2001) proposed a local Gabor-based approach in which the Gabor filters were determined by using local information. Jin et al. (2004) integrated wavelet and Fourier–Mellin transform to produce a translation, rotation and scale invariant feature. Although these algorithms can solve the problem shown in Fig. 1, it is difficult to achieve the matching process when the reference point is missing.

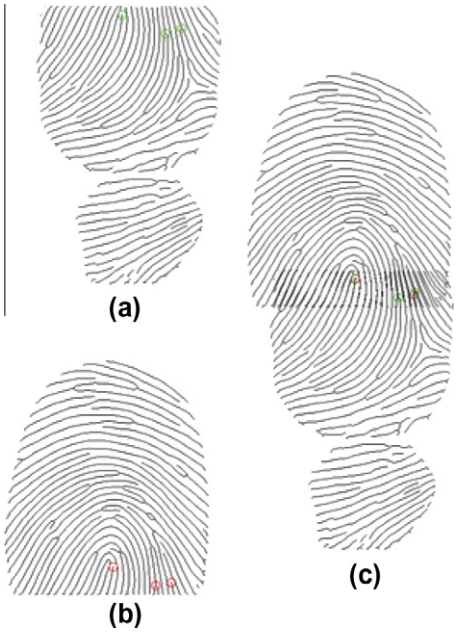

Fig. 2. An example of a pair of fingerprints from FVC2002 DB1 with a small overlapping region: (a) thinned image of 29_6.tif; (b) thinned image of 29_7.tif; (c) registration of (a) and (b).

Minutiae-based algorithms cannot characterize the overall ridge pattern of the fingerprint, whereas reference point-based global features are very sensitive to the accuracy of the reference point detection. It is desirable to explore robust fingerprint representation schemes which combine global and local information in a fingerprint to reinforce the individuality of fingerprints. Gu et al. (2006) proposed to combine the global structure (orientation field) and local cues (minutiae) to represent a fingerprint. Similarities based on the orientation field and minutiae were fused in the decision level to calculate the matching score. However, this method has the same shortcomings as the minutiae-based matchers that overlapping regions of different fingers may possess a similar orientation field, as shown in Fig. 1. Inspired by the conclusion that integration at the feature level provides better recognition results than other levels of integration (Jain et al., 2005), we propose a minutiae-based fingerprint matching algorithm by incorporating the global knowledge into minutiae descriptor. The contributions of our paper include: first, the reference point detection algorithm is improved and some additional checking conditions are added to ensure that accurate and genuine reference points can be found. Second, minutia handedness, which is determined by its associated ridges or the position of the reference points, is proposed to improve the matching performance. The proposed algorithm is tested on eight data sets of FVC2002 (2002) and FVC2004 (2004). The experimental results indicate that the performance of a convectional fingerprint recognition algorithm can be improved by incorporating minutia handedness.

The rest of this paper is organized as follows. Section 2 gives the definition of the feature of minutia handedness. Section 3 describes our matching algorithm with minutia handedness. Experimental results are reported in Section 4. Finally, the conclusions are drawn in Section 5.

2. Minutia handedness

In this section we introduce a novel feature called minutia handedness to capture global knowledge. It is defined for each minutia according to the bending degree of its associated ridge or the position of the reference points. Three types of minutiae handedness are defined in this paper: right-handed, left-handed and non-handed. A right-handed minutia means that all the reference points are on the right side of the minutia if we stand on the minutia point and turn our face to the minutia direction. Similarly, a left-handed minutia means that all of the reference points are on the left side of the minutia. Non-handed minutia means that the handedness cannot be determined for it. However, some fingerprint images may miss the reference point and the position of the reference point may be affected by noise. In this paper, we use the property that ridges generally bend backwards to the reference point is utilized to cover the shortage of an inaccurate reference point. If the ridge associated with a minutia has a large bending degree, the minutia handedness is determined by its associated ridge, otherwise by the reference point.

2.1. Minutia handedness determination by associated ridges

We first present the representation of the ridges associated with a minutia. Two widely used types of minutiae are ridge ending and ridge bifurcation. For a ridge ending, it has only one associated ridge. The ridge is sampled every qth point, and it is represented as $P = \{p_i = (x_i, y_i)\}_{i=1}^{n_p}$ as shown in Fig. 3(a), where n_p denotes the number of sampling points and p_1 denotes the ridge ending. As for a ridge bifurcation, it has three associated ridges and each ridge is first sampled starting from the minutia. In order to simplify the calculation, the two nearest ridges surrounding the angle of the

bifurcation are averaged to generate a virtual ridge. Thus, the virtual ridge and the remaining real ridge are connected to generate a new ridge as shown in Fig. 3(b). Similar to ridge ending, the sampling point set can also be represented as $P = \{p_i = (x_i, y_i)\}_{i=1}^{n_p}$, where n_p is the total number of the sampling points. It is worth noting that the points are ordered according to the minutia's direction. For a minutia M, its handedness determination is described as follows.

In this paper, the height of the ridge is used to measure its bending degree. Let A and C denote the first and the last points, respectively, of the ridge P ($A = p_1$ and $C = p_{n_p}$). The height of the ridge P is defined as the maximal distance from the point set P to the line AC that connects A and C. Let B denote the point that maximizes the distance and D denote the projection point of B on the line AC, then the length of BD (i.e. $|BD|$) is the height of the ridge, as shown in Fig. 9. If $|BD|$ is larger than the threshold $H_T(n_p)$, which is a monotone increasing function of the total sampling number n_p, then ridge P is regarded as having adequate bending and the minutia handedness of M can be determined by it.

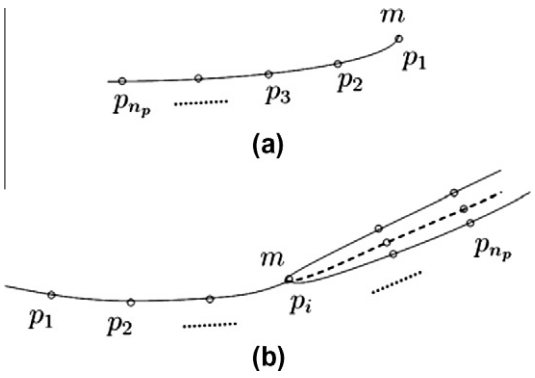

Fig. 3. Ridge representation: (a) ridge ending; (b) ridge bifurcation.

For a triangle ΔABC, its area $S_{\Delta ABC}$ with a sign is calculated as 1/2 times the value of a determinant (O'Rourke, 1988), known as

$$S_{\Delta ABC} = \frac{1}{2}\begin{bmatrix} x_A & y_A & 1 \\ x_B & y_B & 1 \\ x_C & y_C & 1 \end{bmatrix} = \frac{1}{2}(x_B - x_A)(y_C - y_A) - \frac{1}{2}(x_C - x_A)(y_B - y_A) \tag{1}$$

From the above formula, the minutia handedness can be easily obtained. It is regarded as right-handed if $S_{\Delta ABC} < 0$, otherwise left-handed.

On the other hand, if ridge P is not bending adequate, the minutia handedness of M cannot be determined by P. In this case, it is defined based on the reference point. If no reference point is available, then the minutia handedness of M is set as being non-handed, otherwise, it is determined by the relation between the ridge and the reference point.

2.2. Minutia handedness determination by the reference point

2.2.1. Reference point detection

Before detecting the reference point, the orientation field of the input fingerprint image of $H \times W$ pixels is computed by the approach proposed by Bazen and Gerez (2002). In order to improve the efficiency of the detection, the pixel-wise orientation field is divided into $(H/w) \times (W/w)$ blocks of grid size w and the block orientation field O is obtained by using average orientation. The reference point detection is based on the block orientation field. Two types of reference points are used in this work: core point and the point of maximum curvature in concave or convex ridges (MC point for short).

We will first discuss core point detection. There are several techniques to detect singular points (Novikov and Kot, 1998; Kawagoe and Tojo, 1984; Nilsson and Bigun, 2003; Wang et al., 2007b) in fingerprints. In this paper, we adopt complex filtering (Nilsson and Bigun, 2003), which provides not only the position but also the angle of a singular point, to detect the core point.

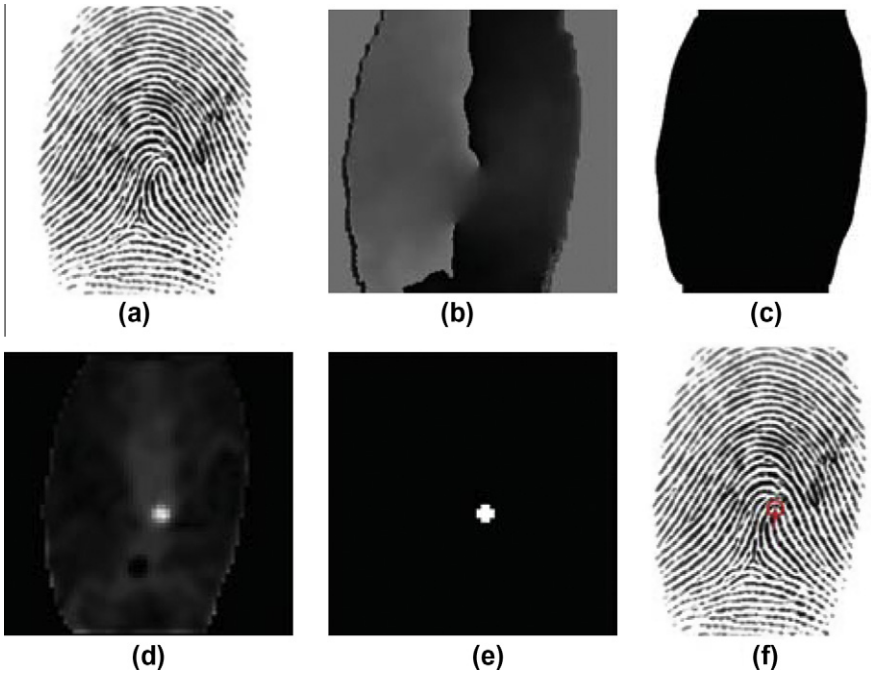

Fig. 4. Illustrations of core point detection: (a) original fingerprint image (1_1.tif from FVC2002 DB1); (b) orientation image; (c) foreground mask; (d) core-certainty map on the block orientation field ($w = 6$); (e) binarization of the core-certainty map ($\mu_T = 0.45$); (f) fingerprint image with the core point and its orientation. (d) and (e) are resized to obtain better visual effects.

The orientation tensor over the block orientation field is obtained by the following equation

$$z = \cos(2\theta) + i\sin(2\theta) \tag{2}$$

where θ is the block orientation field. Convolutions between orientation tensor and symmetry filters (Nilsson and Bigun, 2003) result in two certainty responses: z_{core} and z_{delta}. The following approach is adopted to sharpen the magnitude of the core point responses (Nilsson and Bigun, 2003):

$$\mu_{core} = |z_{core}|(1 - |z_{delta}|) \tag{3}$$

The centroid of each region, where the certainty measure is larger than the prefixed threshold μ_T, is regarded as a core point candidate, and the average angle of the z_{core} in this region is viewed as the angle of the corresponding candidate. Fig. 4 illustrates the core point detection process.

Note that there may be false candidates in a fingerprint. The following three operations are proposed to remove them:

(1) Based on the observation that the region opposite to the angle of the core point possesses a large curvature, we take the candidate with small a curvature as a false one. The geometry of regions R_1 and R_2 (Jain et al., 1999), as shown in Fig. 5, is adopted to capture the curvature. For each candidate, the geometry is transformed to ensure that its angle and centre coincide with the angle and position of the candidate respectively. The curvature measure $\mathcal{D}$ is computed by the following formula:

$$\mathcal{D} = \sum_{R_1'} |\cos(O_{k,l} - \theta_c)| - \sum_{R_2'} |\cos(O_{k,l} - \theta_c)| \tag{4}$$

where θ_c is angle of the core candidate, $O_{k,l}$ is the orientation at point (k,l), and R_1' and R_2' are the transformed versions of R_1 and R_2 respectively. If $\mathcal{D}$ is less than the threshold $\mathcal{D}_T$, i.e. $\mathcal{D} < \mathcal{D}_T$, then this candidate is set as being false and is removed from the candidate set.

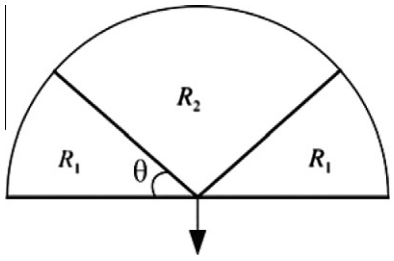

Fig. 5. Semi-circle mask (Jain et al., 1999) for false core point removal and MC point detection. The arrow points to the angle of the mask.

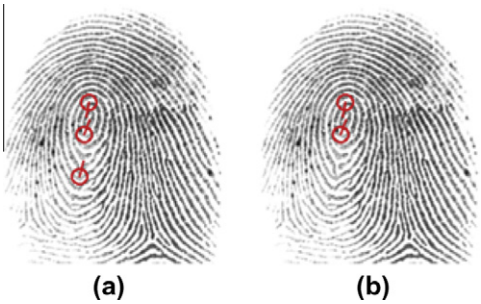

Fig. 6. An instance on 54_1.tif from FVC2002 DB1: (a) detected core points; (b) after the removal of the false core point.

(2) For some images with noise in the high curvature regions, there may be two similar candidates. Assuming that θ_a and θ_b are the angle of core point candidates a and b respectively, θ_{ab} is the orientation of the line connecting a and b. a and b are considered to be similar if they satisfy the following three conditions: (1) $\lambda_1(\theta_a,\theta_b) < \theta_T$, (2) $\lambda_2(\theta_a,\theta_{ab}) < \theta_T$, and (3) $\lambda_2(\theta_b, \theta_{ab}) < \theta_T$, where $\lambda_1(\theta_1,\theta_2)$ is the angle distance between θ_1 and θ_2, $\lambda_2(\theta_1,\theta_2)$ is the orientation distance between θ_1 and θ_2, and θ_T is the threshold. Since the core point is defined as the topmost point on the innermost upward recurving ridgeline of fingerprint (Srinivasan and

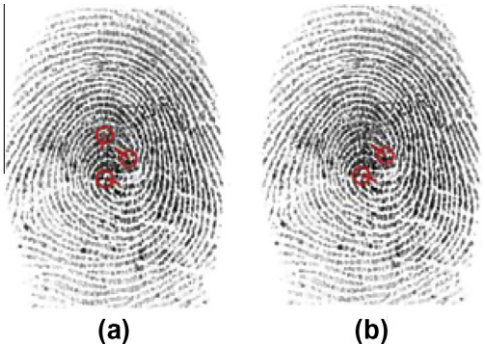

Fig. 7. An instance on 97_1.tif from FVC2002 DB1: (a) detected core points; (b) after the removal of the false core point.

Fig. 8. Four instances in MC point detection. Green circle denotes the detected MC point. (a) a partial fingerprint from the fingertip and MC point (FVC2002 DB1 1_5.tif); (b) a complete arch-type fingerprint image and MC point (FVC2002 DB1 70_1.tif); (c) a partial fingerprint from the fingerbottom and MC point (FVC2002 DB1 39_5.tif); (d) a fingerprint without a reference point (FVC2002 DB1 29_6.tif). (For interpretation of the references to colour in this figure legend, the reader is referred to the web version of this article.)

Murthy, 1992), the candidate, which points to the other one is judged as a false one and removed from the candidate set. Fig. 6 exemplifies this case.

(3) If the number of candidates is still larger than two after performing the two operations above, one more operation is needed to select the core points. If the maximal angle distance between any pair is larger than the threshold ($3\pi/4$ in our experiment), meaning they have opposite orientation directions, then the corresponding pair of candidates are selected as the final core points. Fig. 7 illustrates this case. Otherwise, all of the candidates are regarded as false ones.

It cannot be guaranteed to find a core point in every fingerprint image. For instance, there is no core point in arch-type fingerprint images or some partial fingerprint images. Jain et al. (1999) proposed the sine-map-based method and the geometry of regions R_1 and R_2 to capture the maximum curvature in concave ridges. Chan et al. (2004) enhanced this approach with some additional checking conditions. Here, we improve their approach to calculate the difference of the sine component between region R_1 and R_2 (D) and the continuity of a possible reference point (C). For further details, we refer the readers to Chan et al. (2004). In order to detect a stable MC point and avoid a false MC point, the point (k,l) satisfying the following two conditions is selected as a MC point candidate: (1) $D_{k,l} > D_{thr}$, (2)$C_{k,l} > C_{thr}$. The first condition ensures that the candidate must possess a large curvature while the second one ensures that there are a certain number of concave ridges upon the detected MC point, thus reducing impact of the noise in the orientation field. The point with the largest y coordinate in the candidate set is selected as the MC point on the concave ridges. Afterwards, the orientation field is flipped upside down and the above procedure is conducted once again to capture the MC point on the convex ridges. Fig. 8 presents four results in the MC point detection process.

2.2.2. Minutia handedness determination

Reference points are used to determine the minutia handedness in this section. Let $R = \{r_j = (x_j, y_j)\}_{j=1}^{n_r}$ denote the reference point set, where n_r denotes the number of the reference points. For each reference point $E = r_j$, A, E and C form a triangle. The sign of $S_{\Delta AEC}$ demonstrates the position of E relative to the line AC. If all of the reference points are on the same side of the line AC, that means all of the corresponding triangles have the same sign, then the minutia handedness of this minutia can be determined by the reference point set. Different from Section 2.1, the minutia handedness of M is set as being right-handed if $S_{\Delta AEC} > 0$, left-handed otherwise. In practice, noise may impact the position of the reference points and then result in incorrect minutia handedness. Therefore, if the minimal distance from the reference point set to the line AC or the minimal distance between the minutia and the reference point set is less than the threshold, the minutia handedness of M is regarded as being non-handed. Fig. 9(d) gives an instance satisfying one of these conditions. Fig. 9 exemplifies the process of minutia handedness determination.

Handedness of a minutia is first judged by its associated ridge. If the ridge does not bending enough, then the handedness depends on the reference point. That means minutia handedness is first determined by ridge and then reference point, and there will not be a conflict. It is also worth noticing that the determination sequence cannot be exchanged. The reason lies in that for a minutia with a very height ridge, the reference point and point B may be on

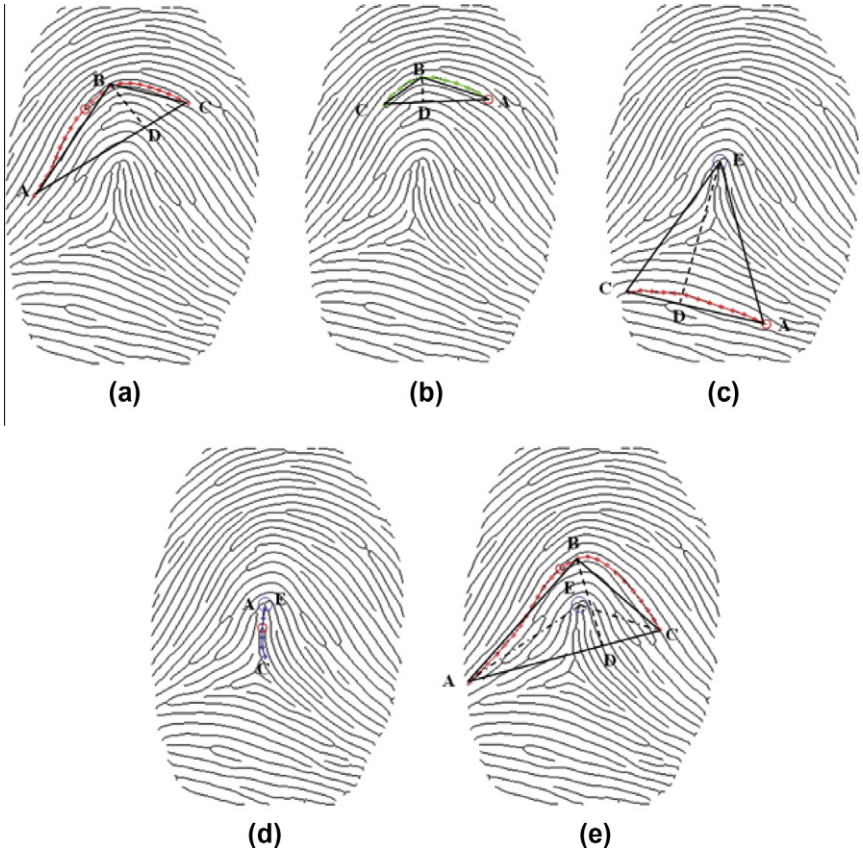

Fig. 9. Illustration of minutia handedness determination. (a) a right-handed minutia determined by its associated ridge; (b) a left-handed minutia determined by its associated ridge; (c) a right-handed minutia determined by the reference point; (d) an instance that the minutia handedness cannot be determined by the reference point; and (e) an instance the minutia handedness results from its associated ridge is opposite to that results from the reference point.

Table 1
Minutia handedness type matching rules.

Type of verification minutia	Match with type of reference minutia
00	00, 01, 10
01	00,01
10	00,10
01 = right-handed, 10 = left-handed, 00 = non-handed	

the same side of the line *AC*. In this case, the minutia handedness obtained from Section 2.1 is opposite with that obtained from Section 2.2 and the former one gives the right minutia handedness. Fig. 9 (e) exemplifies this case. Minutia handedness is a rotation and translation-invariant feature. Right-handed minutiae are hardly mistaken for being left-handed and vice versa, even if severe distortion exists in a fingerprint image. Table 1 gives the matching rules. According to the matching rules, two minutiae are regarded as non-matchable if and only if one of them is right-handed and the other is left-handed, otherwise, they are matchable.

3. Matching method with minutiae handedness

Since minutia handedness can be embedded into any minutiae-based fingerprint matching algorithm, we embed it into the orientation descriptor proposed by Tico and Kuosmanen (2003) for the matching performance evaluation. The descriptor comprises the orientation information at the same sampling points around the minutia point in a circular pattern. The circular pattern consists of L concentric circles of radii r_l, each one comprises of K_l sampling points $p_{k,l}$, which are equally distributed along their circumference. Let $a = \{\alpha_{k,l}\}$ and $b = \{\beta_{k,l}\}$ denote two minutiae descriptors. The similarity between a and b is computed as

$$S_{ab} = 1/K \sum_{l=1}^{L} \sum_{k=1}^{K_l} s(\lambda_1(\alpha_{k,l}, \beta_{k,l})) \tag{5}$$

where $K = \sum_{l=1}^{L} K_l$, $\lambda_1(\alpha_{k,l},\beta_{k,l})$ is the orientation distance between angles $\alpha_{k,l}$ and $\beta_{k,l}$, and $s(x)$ denotes a similarity value with respect to the angle x. However, this similarity measure is prone to pair two minutiae with a large number of valid sampling point. In Feng (2008), Feng proposed to use the mean similarity value of valid corresponding sampling points to compute the similarity S_{ab}.

$$S_{ab} = mean(s(\lambda_1(\alpha_{k,l}, \beta_{k,l}))) \tag{6}$$

In this paper, we take the minutia handedness into account. The formula used to calculate the similarity is expressed as follows,

$$S_{ab} = \begin{cases} mean(s(\lambda_1(\alpha_{k,l}, \beta_{k,l}))) & \text{if } a \text{ and } b \text{ are matchable} \\ 0 & \text{otherwise} \end{cases} \tag{7}$$

We use the same sampling structures and parameters as in Feng (2008).

Let $\{p_k\}_{k=1}^{N_p}$ and $\{q_l\}_{l=1}^{N_q}$ denote two minutiae sets from the template fingerprint and the input fingerprint respectively, and $\{S_{kl}\}_{k=1,l=1}^{N_p,N_q}$ denote the set of similarities between each minutiae pair. In the matching process, $\{S_{kl}\}_{k=1,l=1}^{N_p,N_q}$ is first rearranged in a decreasing order and the top N_t minutiae pairs are used as initial minutiae pairs for alignment attempt. The alignment-based greedy matching algorithm (Feng, 2008) is used to establish the minutiae correspondences, and finally, the following formula is used to calculate the score.

$$score = \begin{cases} \frac{2\sum_{k=1}^{n} S_{p_k q_k}}{q+t+M} & \text{if } n > n_{Thr} \\ 0 & \text{otherwise} \end{cases} \tag{8}$$

where $\{(p_k, q_k)\}_{k=1}^{n}$ is the matched minutiae pair set, q and t are the number of minutiae located inside the two fingerprint overlapping regions for the template fingerprint and the input fingerprint respectively, and M is a bias parameter balancing FMR and F NMR. The largest score in the N_t attempts is selected as the matching score.

4. Experimental results

In order to show the effectiveness of the proposed approach, we evaluate both the accuracy of the core point detection and the performance of the global knowledge-minutia handedness incorporation strategy. The proposed algorithm has been evaluated on the databases provided by FVC2002 and FVC2004, where each database contains 800 fingerprints from 100 different fingers. The total number of genuine matches for calculating the false non-match rate (F NMR) is $100C_8^2 = 2800$. The total number of imposter matches for calculating the false match rate (FMR) is $C_{100}^2 = 4950$. More details about the databases and the protocol are available in these websites (FVC2002, 2002; FVC2004, 2004). All of the experiments are conducted on the same PC with an Intel Pentium 4 processor 3.4 GHz

Table 2
Performance of the proposed core point detection algorithm compared with (Chikkerur and Ratha, 2005).

	Proposed	Chikkerur and Ratha (2005)
False core point	18 (of 955)	74 (of 955)
Missed core point	30	11

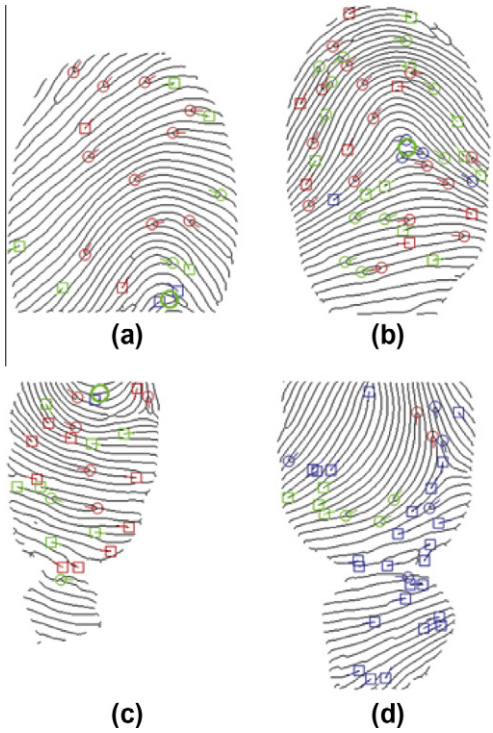

Fig. 10. Instances of minutia handedness detection (red denotes right-handed, green denotes left-handed and blue denotes non-handed; circle denotes ridge bifurcation and square denotes ridge ending: (a) a partial fingerprint from the fingertip (FVC2002 DB1 1_5.tif); (b) a complete arch-type fingerprint image (FVC2002 DB1 70_1.tif); (c) a partial fingerprint from the fingerbottom (FVC2002 DB1 39_5.tif); and (d) a fingerprint without a reference point (FVC2002 DB1 29_6.tif). (For interpretation of the references to colour in this figure legend, the reader is referred to the web version of this article.)

under the Windows XP professional operating system. We provide the value of the parameters used during the matching process: grid size of the orientation field ($w = 6$), radius and angle of the semi-circle mask ($R = 8$, $\theta = \pi/4$), thresholds for reference point detection ($\mu_t = 0.45$, $C_{thr} = 8$, $D_T = D_{thr} = 12$, $\theta = \pi/4$), and the sampling interval ($q = 10$ pixels). We obtain the ridge height threshold by the following piecewise function:

$$H_T(n) = \begin{cases} 8 & \text{if } n < 5 \\ 1.5 \cdot n & \text{otherwise} \end{cases} \quad (9)$$

All of the experiments in this section share the same parameters.

4.1. Accuracy of core point detection

An experiment is conducted on FVC2002 DB1 to evaluate the accuracy of core point detection. We manually marked the core point positions and a total of 955 core points were obtained. As described in Chikkerur and Ratha (2005), the detected core point is considered to be false if the position is more than 30 pixels from the marked location. The comparison between the proposed algorithm and (Chikkerur and Ratha, 2005) is given in Table 2. Compared with (Chikkerur and Ratha, 2005), although the number of missed core points is slightly increased, the number of false core points decreases by 76%. This indicates that the checking conditions are effective to diminish the false core points.

4.2. Accuracy of minutia handedness detection

To demonstrate the accuracy of minutia handedness detection, we make the following conventions: (1) the handedness of a minutia is said to be incorrectly detected if a right-handed minutia is mistaken as a left-handed one or a left-handed minutia is mistaken as a right-handed one; (2) the handedness of a minutia is said to be correctly detected if its handedness is not non-handed and not incorrectly detected. All of the minutiae and their handedness in the fingerprint images in Fig. 8 are drawn in Fig. 10, where red denotes right-handed, green is left-handed and blue is non-handed. We label these fingerprints in Fig. 8(a)–(d) as fingerprint 1, 2, 3

Table 3
Accuracy of minutia handedness detection.

Fingerprint	Minutiae number	Correct rate (%)	Incorrect rate (%)	Non-handed rate (%)
1	21	90.5	0.0	9.5
2	48	89.6	0.0	10.4
3	25	96	0.0	4
4	39	23.1	0.0	76.9
5	60	90	3.3	6.7
6	24	91.7	0.0	8.3
7	60	76.7	18.3	5
8	46	71.7	0.0	28.3
summary	323	77.4	4.0	18.6

Table 4
Percentage of minutiae which handedness is determined by its associated ridge.

Data set	FVC2002 DB1	FVC2002 DB2	FVC2002 DB3	FVC2002 DB4
Percentage	24.6%	25.0%	24.7%	21.4%
Data set	FVC2004 DB1	FVC2004 DB2	FVC2004 DB3	FVC2004 DB4
Percentage	21.6%	22.3%	20.9%	18.9%

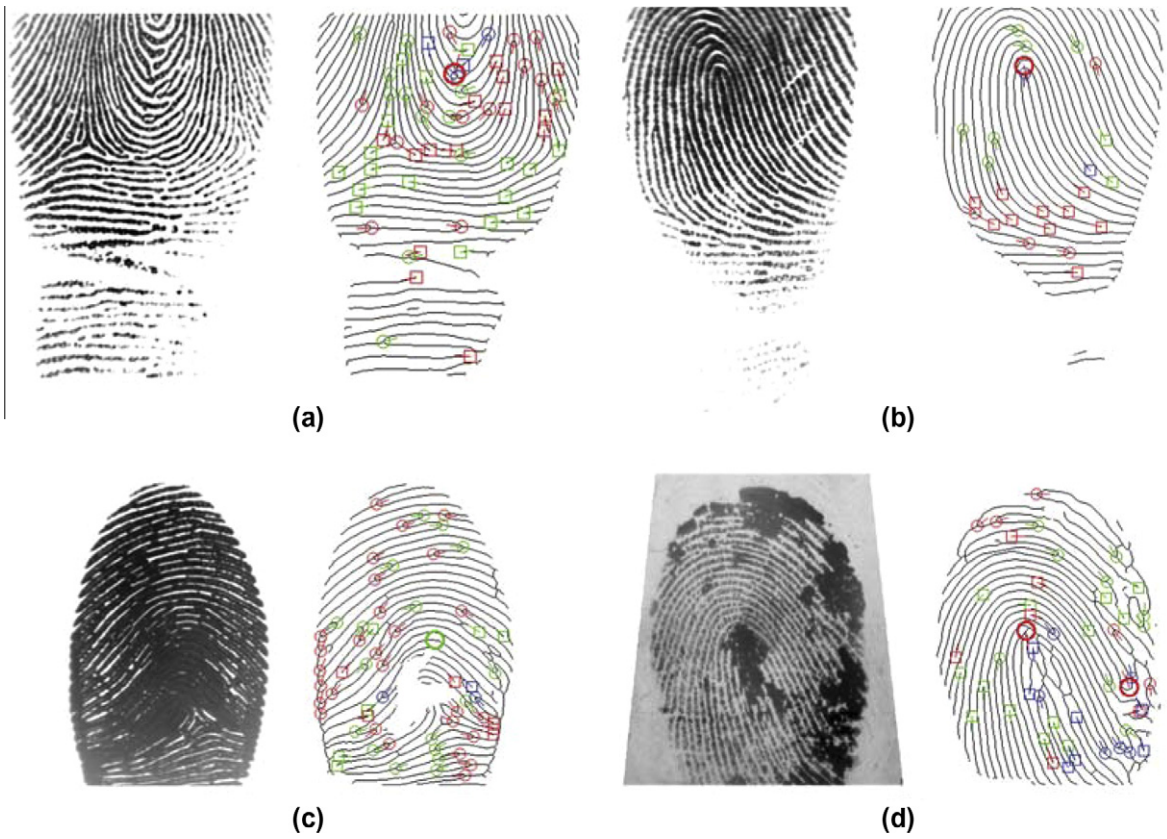

Fig. 11. Instances of minutia handedness detection: (a) 54_5.tif from FVC2002 DB1; (b) 34_1.tif from FVC2004 DB1; (c) 99_8.tif from FVC2004 DB1; and (d) 58_8.tif from FVC2004 DB2.

Table 5
Number of fingerprints with reference point on FVC2002 and FVC2004.

Data set	FVC2002 DB1	FVC2002 DB2	FVC2002 DB3	FVC2002 DB4
No.	787	781	782	752
Percentage	98.4%	97.6%	97.8%	94.0%
Data set	FVC2004 DB1	FVC2004 DB2	FVC2004 DB3	FVC2004 DB4
No.	794	790	797	697
Percentage	99.3%	98.8%	99.6%	87.1%

and 4 respectively. Another four instances are presented in Fig. 11, in which the four fingerprints are labeled 5, 6, 7 and 8 respectively. The accuracy of minutia handedness detection on these 8 fingerprints is reported in Table 3. The images of Fig. 10(a)–(c) indicate that the handedness of all of the minutiae are correctly detected. In Fig. 10 (d), where no reference point is available, the handedness of 9 minutiae (7 left-handed minutiae and 2 right-handed minutiae) is correctly detected by using stage 1. Fig. 11(d) illustrates an example of a fingerprint image of low quality in which two core points are detected and one of them is false. In this case, two left-handed minutiae between two core points are correctly detected and no minutia handedness is incorrectly detected. Stage 1 is used to obtain right minutia handedness by its associated ridge and reduce the negative effect of the false or absent reference point. Stage 1 is more reliable than Stage 2. However, no more than 25% minutiae handedness is determined by the ridge in the overall databases (as shown in Table 4). On the contrary, on average 96% fingerprints in FVC2002 and FVC2004 have detected reference points (as shown in Table 5). Therefore, Stage 2 is a necessary step in minutia handedness calculation. The requirement in Stage 2 that minutia handedness can be defined only when all of the reference points on the same side also aims to reduce the effect of the false reference point. This example indicates that minutia handedness is difficult to incorrectly detect as long as a true reference point exists. In Fig. 11(c), the MC point is about 70 pixels away from the position of the core point. Therefore, the inaccurate MC point results in the wrong type of minutia handedness of the 11 minutiae.

4.3. Matching performance evaluation

In order to validate the performance of the proposed algorithm (Algorithm C), we also implement two related algorithms (Algorithm A and Algorithm B). The only difference between Algorithm A and Algorithm C is that Algorithm A uses formula (6) to calculate minutiae similarity whereas Algorithm C uses formula (7). The difference between Algorithm B and Algorithm C is the matching score computation. An additional alignment checking approach, which is based on core points is added in Algorithm B. An alignment attempt is regarded as being correct only if two fingerprints satisfy one of the following three conditions:

(1) At least one of these fingerprints does not have a core point.
(2) There exists a pair of core points whose direction is opposite (larger than $3\pi/4$).

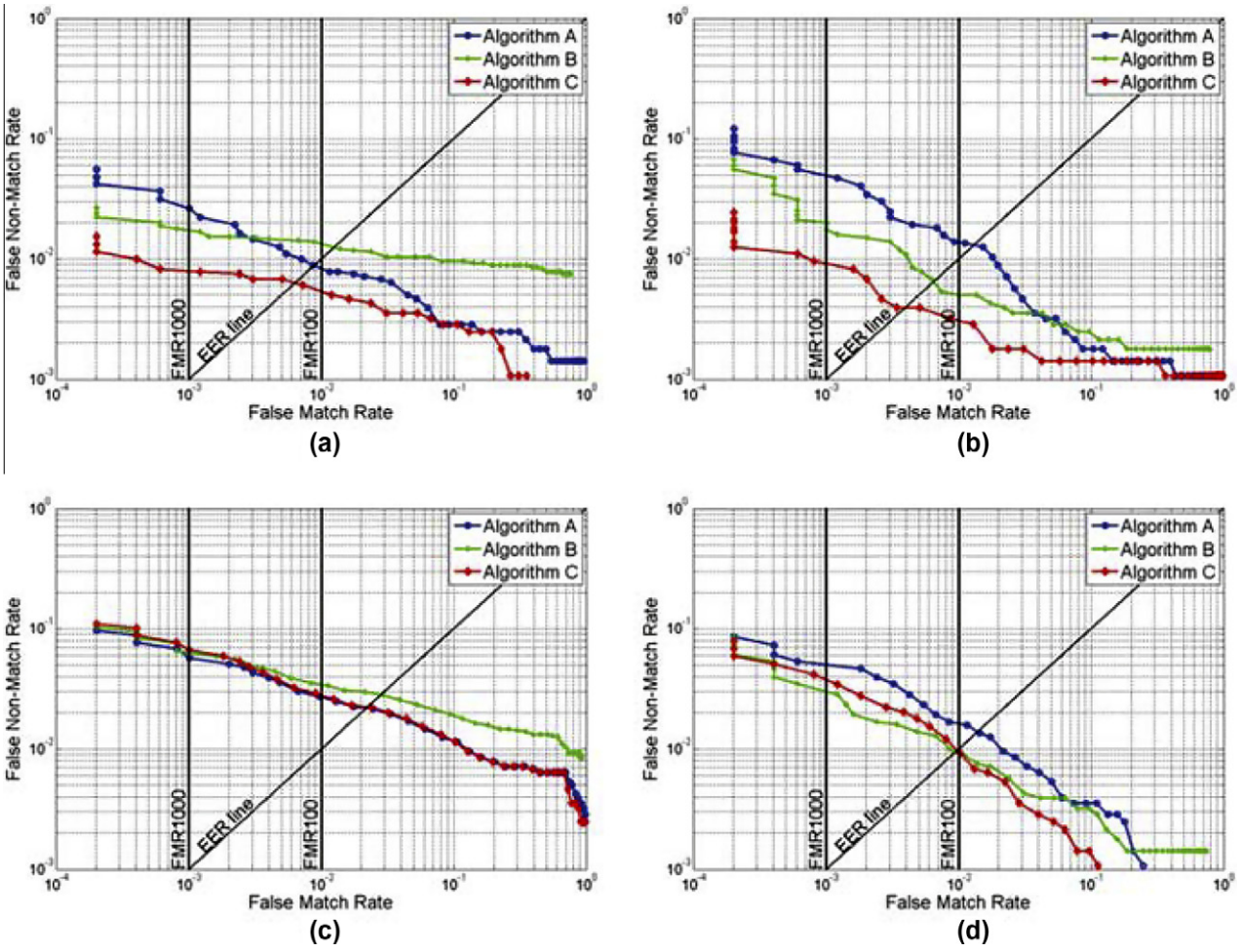

Fig. 12. ROC curves over FVC2002. (a) DB1; (b) DB2; (c) DB3 and (d) DB4.

(3) There exists a pair of core points that are close in position (less than 40 pixels) and the difference of their direction is minor (less than $\pi/4$).

Matching score of an incorrect alignment attempt is directly set to zero.

The receiver operating characteristic (ROC) curves of these algorithms over the eight databases are plotted in Figs. 12 and 13 in log–log scales. The performance indices provided by FVC2002 and FVC2004 such as EER, FMR100, FMR1000 and ZeroFMR are reported in Tables 6 and 7. From the ROC curves and the indices, we can see that Algorithm C obviously outperforms the other two. More details are analyzed as follows:

(1) On the data sets in which most fingerprints are complete, i.e. FVC2002 DB1, DB2, DB3 and four data sets of FVC2004, the FNMRs of the proposed algorithm rapidly decrease with respect to their FMRs. Matching rules of minutia handedness make the alignment of the two fingerprints from a global perspective, which rejects most impossible alignments. In Fig. 1 core point detection over FVC2002 DB1 56_1.tif misses its core point, whereas MC point is detected accurately. Using Eq. (6), the matching score between these two fingerprints is 0.535, while the similarity threshold at EER point is about 0.459. However, using the Eq. (7), the alignment in Fig. 1(c) does not occur. The matching score of these two fingerprints is reduced to 0.101, while the similarity threshold at EER point is about 0.403. It proves that minutia handedness can effectively reduce the false acceptance rate and then improve the overall performance. However, alignment checking does not reject such imposter matches. The matching score of Algorithm B over these two fingerprints is still 0.535. This indicates that alignment checking cannot deal with fingerprints of the arch type or fingerprint images without a core point. Therefore, over some data sets, ZeroFMRs of Algorithm B are much larger than that of Algorithm C.

(2) Although there are 18 false core points in the FVC2002 DB1, as reported in Table 2, the performance of Algorithm C is still greatly improved. The EERs of Algorithm A and Algorithm C are 0.90% vs. 0.64%. Their FMR100s, FMR1000s and ZeroFMRs are 0.78% vs. 0.54%, 2.75% vs. 0.78% and 5.89% vs. 1.71% respectively. This is because the minutia handedness is robust to false and missing reference points. In stage 1, the handedness of a minutia with a very height ridge is only determined by its associated ridge. It could be correctly estimated even if there were false reference points or no reference point. In stage 2, the minutia handedness can be determined if all of the reference points are on the same side of the line. This operation does not have any adverse effects on the accuracy of the match as long as true reference points exist. As reported in Table 3, even when true core points are missed and false core points are detected, most minutiae can be classified correctly because false core points also possess a large curvature and are near fingerprint center. However,

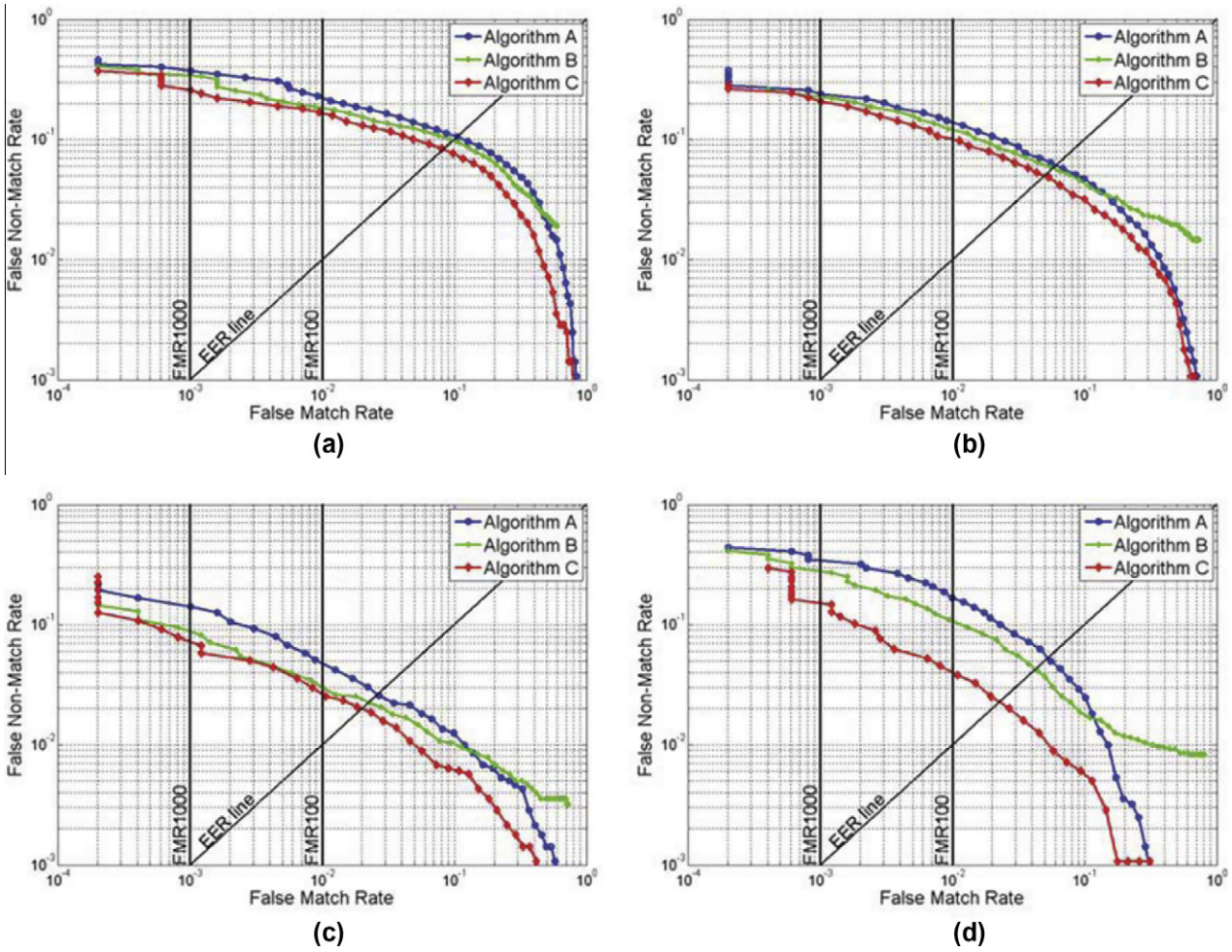

Fig. 13. ROC curves over FVC2004. (a) DB1; (b) DB2; (c) DB3 and (d) DB4.

Table 6
Performance of the three algorithms on FVC2002.

Data set	Algorithm	EER (%)	FMR100 (%)	FMR1000 (%)	ZeroFMR (%)
DB1	A	0.90	0.78	2.75	5.89
	B	1.29	1.32	1.71	2.78
	C	0.64	0.54	0.78	1.71
DB2	A	1.25	1.39	5.14	12.54
	B	0.64	0.50	2.03	6.64
	C	0.40	0.32	0.93	2.64
DB3	A	2.18	2.68	5.89	10.21
	B	2.80	3.39	6.29	10.89
	C	2.22	2.86	6.86	11.79
DB4	A	1.39	1.64	5.25	9.36
	B	0.93	0.89	3.11	9.36
	C	0.93	0.93	3.82	8.54

Table 7
Performance of the three algorithms on FVC2004.

Data set	Algorithm	EER (%)	FMR100 (%)	FMR1000 (%)	ZeroFMR (%)
DB1	A	10.48	22.54	37.42	45.89
	B	9.72	18.21	34.43	41.61
	C	8.26	16.79	26.00	38.68
DB2	A	6.16	13.89	24.06	40.14
	B	5.80	11.89	22.89	27.21
	C	4.97	9.93	21.50	28.54
DB3	A	5.29	16.61	34.39	45.07
	B	4.22	10.64	29.07	43.07
	C	2.32	4.04	14.64	31.89
DB4	A	2.58	5.04	15.00	22.00
	B	2.26	2.96	9.21	22.14
	C	2.00	2.68	6.64	25.60

Algorithm B heavily depends on the accuracy of core point detection. A false core point such as in Fig. 11(a) may result in 7 false rejections. When core points are missed, MC point is taken as reference point in Algorithm C, and minutia handedness also takes effect. However, if the MC point is taken into alignment checking in Algorithm B, its performance will be worse (large variation in partial fingerprints and low quality fingerprints).

(3) From Fig. 12(c), we can see that the ROC curves of Algorithm A and Algorithm C over FVC2002 DB3 are very close. Three indices (EER, FMR100 and FMR1000) of Algorithm C are slightly higher than in Algorithm A. Many fingerprint images from FVC2002 DB3 are incomplete and captured only the region around or upper the center of the finger. In this case, the orientation descriptor is capable in finding the best alignment from a global perspective and this incorporation scheme seems to provide no assistance for fingerprint matching.

The average matching times of Algorithm C over the four databases of FVC2002 are 7.62 ms, 13.07 ms, 3.44 ms and 5.32 ms respectively. Over the four databases of FVC2004, the figures are 8.23 ms, 7.10 ms, 12.60 ms and 9.06 ms respectively. The average matching times of Algorithm C are shorter than in Algorithm A because similarities between non-matchable minutiae do not need to be calculated and are set to zero directly, the difference is less than 0.2 ms.

5. Conclusion and discussion

The primary contribution of our approach is that it takes the global knowledge into account. Minutia handedness is proposed to capture the global knowledge. As long as a true reference point exist, the false reference has less effect on the matching performance. The experimental results proved the proposed method can improving matching performance efficiently. Since there are only three types of minutiae handedness, two bits are enough to store the type of minutia handedness. Therefore, the proposed algorithm needs only small additional computational resources. It can be embedded into any minutiae-based fingerprint matching algorithm. However, in FVC2002 DB3, most fingerprints are captured only the region around or upper the center of the finger. Then, the orientation descriptor is capable in finding the best alignment from a global perspective, and the case such as Fig. 1 is hard to occur. Therefore, fingerprint matching does not benefit from minutia handedness. Future work includes analyzing under what conditions it will make the best of minutia handedness and utilizing delta points and/or classification information to further improve the performance and reduce running time.

Acknowledgement

This paper is supported by the National Natural Science Foundation of China under Grant Nos. 60902083, 60803151, 60875018, 61100234, 61101247, Beijing Natural Science Fund under Grant No. 4091004, and the Fundamental Research Funds for the Central Universities.

References

Bazen, A., Gerez, S., 2002. Systematic methods for the computation of the directional fields and singular points of fingerprints. IEEE Trans. Pattern Anal. Machine Intell. 24 (7), 905–919.
Chan, K., Moon, Y., Cheng, P., 2004. Fast fingerprint verification using subregions of fingerprint images. IEEE Trans. Circuits Syst. Video Technol. 14 (1), 95–101.
Chang, J.H., Fan, K.C., 2002. A new model for fingerprint classification by ridge distribution sequences. Pattern Recognit. 35 (6), 1209–1223.
Chen, X., Tian, J., Yang, X., 2006. A new algorithm for distorted fingerprints matching based on normalized fuzzy similarity measure. IEEE Trans. Image Process. 15 (3), 767–776.
Chikkerur, S., Ratha, N., 2005. Impact of singular point detection on fingerprint matching performance. In: AUTOID '05: Proceedings of the Fourth IEEE Workshop on Automatic Identification Advanced Technologies. pp. 207–212.
Feng, J., 2008. Combining minutiae descriptors for fingerprint matching. Pattern Recognit. 41 (1), 342–352.
FVC2002, 2002. http://bias.csr.unibo.it/fvc2002/.
FVC2004, 2004. http://bias.csr.unibo.it/fvc2004/.
Gu, J., Zhou, J., Yang, C., 2006. Fingerprint recognition by combining global structure and local cues. IEEE Trans. Image Process. 15 (7), 1952–1964.
He, Y., Tian, J., Luo, X., Zhang, T., 2003. Image enhancement and minutiae matching in fingerprint verification. Pattern Recognition Lett. 24 (9–10), 1349–1360.
He, Y., Tian, J., Li, L., Chen, H., Yang, X., 2006. Fingerprint matching based on global comprehensive similarity. IEEE Trans. Pattern Anal. Machine Intell. 28 (6), 850–862.
He, X., Tian, J., Li, L., He, Y., Yang, X., 2007. Modeling and analysis of local comprehensive minutia relation for fingerprint matching. IEEE Trans. Systems Man Cybernet. Part B: Cybernet. 37 (5), 1204–1211.
Jain, A., Hong, L., Bolle, R., 1997a. On-line fingerprint verification. IEEE Trans. Pattern Anal. Machine Intell. 19 (4), 302–314.
Jain, A., Hong, L., Pankanti, S., Bolle, R., 1997b. An identity-authentication system using fingerprints. P. IEEE 85 (9), 1365–1388.
Jain, A., Prabhakar, S., Hong, L., 1999. A multichannel approach to fingerprint classification. IEEE Trans. Pattern Anal. Machine Intell. 21 (4), 348–359.
Jain, A., Prabhakar, S., Hong, L., Pankanti, S., 2000. Filterbank-based fingerprint matching. IEEE Trans. Image Process. 9 (5), 846–859.
Jain, A., Nandakumar, K., Ross, A., 2005. Score normalization in multimodal biometric systems. Pattern Recognit. 38 (12), 2270–2285.
Jin, A.T.B., Ling, D.N.C., Song, O.T., 2004. An efficient fingerprint verification system using integrated wavelet and fourier-mellin invariant transform. Image Vision Comput. 22 (6), 503–513.
Kawagoe, M., Tojo, A., 1984. Fingerprint pattern classification. Pattern Recognit. 17 (3), 295–303.
Lee, C.J., Wang, S.D., 2001. Fingerprint feature reduction by principal gabor basis function. Pattern Recognit. 34 (11), 2245–2248.
Lee, C., Choi, J., Toh, K.A., Lee, S., 2007. Alignment-free cancelable fingerprint templates based on local minutiae information. IEEE Trans. Systems Man Cybernet. Part B: Cybernet. 37 (4), 980–992.
Maltoni, D., Maio, D., Jain, A., Prabhakar, S., 2009. Handbook of Fingerprint Recognition, second ed. Springer.

Nilsson, K., Bigun, J., 2003. Localization of corresponding points in fingerprints by complex filtering. Pattern Recognition Lett. 24 (13), 2135–2144.
Novikov, S.O., Kot, V.S., 1998. Singular feature detection and classification of fingerprints using hough transform. In: Sixth International Workshop on Digital Image Processing and Computer Graphics: Applications in Humanities and Natural Sciences. Vol. 3346. SPIE, pp. 259–269.
O'Rourke, J., 1988. Computational Geometry in C. Cambridge University Press.
Pankanti, S., Prabhakar, S., Jain, A., 2002. On the individuality of fingerprints. IEEE Trans. Pattern Anal. Machine Intell. 24 (8), 1010–1025.
Ratha, N., Pandit, V., Bolle, R., Vaish, V., 2000. Robust fingerprint authentication using local structural similarity. In: Fifth IEEE Workshop on Applications of Computer Vision, 2000, pp. 29–34.
Shah, S., Sastry, P., 2004. Fingerprint classification using a feedback-based line detector. IEEE Trans. Systems Man Cybernet. Part B: Cybernet. 34 (1), 85–94.
Srinivasan, V., Murthy, N., 1992. Detection of singular points in fingerprint images. Pattern Recognit. 25 (2), 139–153.
Tico, M., Kuosmanen, P., 2003. Fingerprint matching using an orientation-based minutia descriptor. IEEE Trans. Pattern Anal. Machine Intell. 25 (8), 1009–1014.
Wang, X., Li, J., Niu, Y., 2007a. Fingerprint matching using orientationcodes and polylines. Pattern Recognit. 40 (11), 3164–3177.
Wang, Y., Hu, J., Phillips, D., 2007b. A fingerprint orientation model based on 2d fourier expansion (fomfe) and its application to singular-point detection and fingerprint indexing. IEEE Trans. Pattern Anal. Machine Intell. 29 (4), 573–585.